How to Rotate a Camera

Carlo Tomasi and John Zhang
Computer Science Department, Stanford University
Stanford, CA 94305
{tomasi,zhang}@cs.stanford.edu

Abstract

A procedure is proposed that, given any rotating device to support a camera, places the camera's center of projection to within a tenth of a millimeter from the axis of the rotating device, even with wide angle lenses with severe distortion. Results are experimentally validated by checking that all the camera projection centers as computed through an off-the-shelf calibration method are at the same point in the world, and that the camera rotations computed by the same calibration method are close to the true values measured with a mechanical, high accuracy positioning jig. Experimental data and Matlab code are accessible on the worldwide web.

1. Introduction

In virtually every paper on the analysis of image motion, the motion of the camera is described by a translation of the center of projection and a rotation around it. This choice is made for two reasons. First, placing the origin of the reference system at the center of projection simplifies the equations of perspective projection. Second, rotations around the center of projection provide no parallax, and consequently no three-dimensional information about the scene. Because of this choice, "rotation" is synonym with "rotation around the camera's center of projection," or *central rotation* for short. In any experiment with image motion analysis algorithm, it is then crucial to be able to rotate a camera around its center of rotation, so as to decouple rotation from translation.

Central rotations are important also in practice for the creation of panoramic images. These panoramas are obtained by stitching together images taken by a camera that rotates around its center of projection. The ensuing lack of parallax makes it possible to match adjacent images, at least ideally, by a purely projective transformation of their regions of overlap, without requiring knowledge about the three-dimensional shape of the scene.

We were able to find no method or quantitative accuracy data in the literature about central rotation. This paper proposes a *centering procedure* that, given any rotating device to support a camera, places the camera's center of projection to within a tenth of a millimeter from the axis of the rotating device, even with wide angle lenses with severe distortion. We will make experimental data and Matlab code available on the worldwide web [21].

Sections 2 and 3 explain the principle underlying the camera centering method and the procedure used to determine the accuracy of the results. Section 4 describes the camera model used in this paper, and summarizes the off-the-shelf calibration technique [11, 10] used to determine intrinsic and extrinsic camera parameters. Section 5 shows how point features are localized in the images to provide input to the algorithm, and Section 6 shows experimental results.

2. Achieving Central Rotation

The idea for positioning a camera's center of projection on the rotation axis of a rotation platform is very simple. Figure 1 shows a top view of a camera mounted on a translation stage (the large square), which is itself mounted on top of a rotation stage (the large circle). In the figure, the center of projection of the camera, B, is not on the axis A of rotation of the stage, but is a distance r away from it. The camera sees a nearby target, at distance d, and a far target, at distance D. Both targets are black on the left and white on the right. The near target is lower than the remote target ("lower" here means farther into the page), so both targets are visible from the camera. By moving the near target laterally, its black-to-white transition G is positioned so as to be aligned in the image with the black-to-white transition H of the far target. Figure 4 (c) is the picture seen by the camera in a situation similar to the one in the diagram in figure 1. The dark door and the light wall in the background comprise the far target, and the small black and white card in the foreground is the near target. The translation stage under the camera can be motorized, for an automatic center-

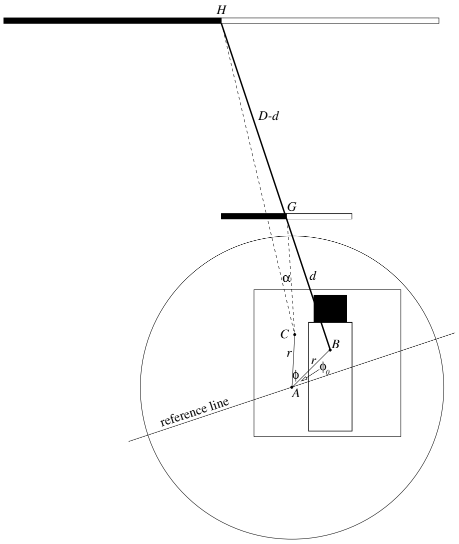

Figure 1. A top view of the rotation centering apparatus. The distance D to the remote target is not to scale.

ing procedure, or manual, as in our setup. The goal of the centering procedure is to move the translation stage until the camera's center of projection B is on the axis of rotation A of the underlying rotation stage.

The principle underlying the centering procedure is that if the rotation axis A and projection center B are separated by a distance r, then as the circular platform rotates, the projection center B describes a circle around A. When a rotation by an angle ϕ moves the projection center to point C, still at distance r from A, the black-to-white transition G of the near target is no longer aligned with that (H) of the far target. Instead, the two transitions are seen at an angle α apart, as shown in Figure 1. Based on the sign of the displacement between the two transition lines, a correction is applied by moving the translation stage so as to bring B closer to A. This procedure can be repeated by applying successively smaller translations that amount to a binary search for the correct position. Once B is along A, rotations of the circular stage cause no displacement between the near and far transition lines, and the procedure terminates.

When H is distant, BH and CH are close to parallel. By the law of cosines for triangles BCG and ABC,

$$\alpha \approx \angle CGB = \arccos \frac{c}{\sqrt{2dc - d^2 + 2r^2(1-\cos\phi)}} \quad (1)$$

where

$$c = d + r\left[\sin\phi_0 - \sin(\phi+\phi_0)\right] \ . \quad (2)$$

The misalignment r between rotation center A and center of projection B is now revealed by α through the angle of

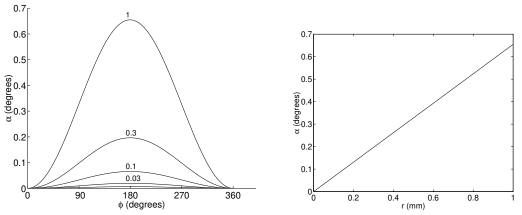

(a) (b)

Figure 2. (a) Image misalignment α as a function of camera rotation angle ϕ for $\phi_0 = 0$ (see figure 1) and for eccentricities $r = 0.01, 0.03, 0.1, 0.3, 1$ mm. (b) Image misalignment α as a function of eccentricity r for $\phi = 180$ degrees and $\phi_0 = 0$.

rotation ϕ. In general this relation depends on the distances d and D to near and far target, and on the initial angular position ϕ_0 of the camera. This initial angular position is measured with respect to a reference line through the rotation center A and orthogonal to the line GH that joins the near and far transitions. The angle ϕ_0 is unknown, and is introduced only for analysis purposes.

Figure 2 shows a plot of the image misalignment angle α as a function of ϕ (with $\phi_0 = 0$) for a set of parameter values that are representative of the situation we encountered in our experiments. More specifically, we used the values $d = 175$ mm and $D = 4500$ mm. From figure 2 (a) we see that an eccentricity r of one tenth of a millimeter produces a maximum image misalignment of about 0.05 degrees at $\phi = 120$ degrees. With a standard 8.8×6.6 mm image sensor and a focal distance of 5.4 mm, as in our experiments, the horizontal field of view is $2\tan(4.4/5.4) \times 180/\pi \approx 120$ degrees, and with 640 pixels per row, 0.05 degrees correspond to $640 \times 0.05/120 \approx 0.27$ pixels, which is close to the limit of accuracy for measuring misalignment (see Section 5). Since 120 degrees is the maximum rotation that can be imparted to the camera while keeping any one point in the field of view at all times, the smallest eccentricity that can be measured with this lens is of the order of one tenth of a millimeter. With narrower fields of view, that is, longer lenses, the misalignment in pixels is larger, and therefore more easily detected.

3. Validation Procedure

The analysis in the previous section shows that with the equipment described therein the centering procedure can position a camera onto a rotating axis with an accuracy of about a tenth of a millimeter. In this section, we describe an experimental procedure to validate this assertion.

The main idea for validation is to apply an extrinsic camera calibration algorithm to several images of an appropriate calibration target (different from the target used in the centering procedure). Between images, the camera is rotated by actuating the rotation platform. The calibration algorithm yields, among other parameters, the pose (position and orientation) of the calibration target with respect to the camera reference system. These results can be inverted by straightforward geometry to yield each of the camera poses in the world reference system. If both the centering procedure and the calibration method are correct, the position of the camera origin should be the same for all the images. In addition, the amounts of rotation between the camera positions should be equal to those returned by the calibration method.

Of course, our validation procedure is adequate only if the camera calibration method can be trusted. For cameras with moderate fields of view, disregarding lens distortion, calibration methods can be found in [6, 7, 3] for fixed intrinsic parameters and in [17, 12, 16] for varying parameters. With controlled camera motion, such as no or known camera translations, these calibration methods can be made more robust [15, 13, 2, 9].

When lens distortion is present, calibration is cast as an optimization problem [20, 11, 19]. In [20], Tsai used a two-stage technique to compute camera position and orientation relative to an object reference coordinate system as well as the effective focal distance, radial lens distortion, and image sensor parameters. Two more steps were added recently [11] to the process by iteratively undistorting the circular patterns for better data accuracy and calibration results. This is the calibration procedure we use in this paper. The performance figures reported by Heikkilä and Silvén [11] are very good. Our experiments in Section 6 can be seen as a combined validation of both our centering procedure and the Heikkilä-Silvén calibration method.

In order to elucidate the validation procedure, consider a right–handed world coordinate system O–XYZ with origin O, placed at some point on the target used in the camera calibration procedure. Let the center of projection of the camera be at C and its coordinate system be C–xyz (also right–handed). The z axis points along the optical axis, and the x and y axes are along rows and columns of the imaging sensor (y points down and x points to the right). Let P be a point which has coordinate components ${}^{w}P = [X, Y, Z]^T$ in O–XYZ and ${}^{c}P = [x, y, z]^T$ in C–xyz. Then

$$ {}^{c}P = {}^{c}_{w}R\,({}^{w}P - {}^{w}C) = {}^{c}_{w}R\,{}^{w}P + {}^{c}O \qquad (3) $$

where ${}^{w}C = [X_c, Y_c, Z_c]$ is the vector of coordinates of C in the world system O–XYZ,

$$ {}^{c}O = -{}^{c}_{w}R\,{}^{w}C \qquad (4) $$

is the vector of coordinates of O in the camera system C–xyz, and ${}^{c}_{w}R$ is the rotation matrix between the two reference systems. If the XYZ Euler angles from O–XYZ to C–xyz are α, β and γ, that is, C–xyz is obtained from O–XYZ by first rotating α around OX, then β around the new Y–axis and finally γ around the newest Z–axis all in the counter-clockwise direction, then ${}^{w}_{c}R = {}^{c}_{w}R^T$ is [4, p. 442]

$$ \begin{bmatrix} c\beta\, c\gamma & -c\beta\, s\gamma & s\beta \\ s\alpha\, s\beta\, c\gamma + c\alpha\, s\gamma & s\alpha\, s\beta\, s\gamma + c\alpha\, c\gamma & -s\alpha\, c\beta \\ -c\alpha\, s\beta\, c\gamma + s\alpha\, s\gamma & c\alpha\, s\beta\, c\gamma + c\alpha\, c\gamma & c\alpha\, c\beta \end{bmatrix} \qquad (5) $$

with the obvious definitions $c\alpha = \cos\alpha, \ldots, s\gamma = \sin\gamma$. This differs slightly from [11] due to different axis conventions. The calibration method in [11] returns the extrinsic parameters

$$ \mathbf{E} = [{}^{c}O, \alpha, \beta, \gamma]^T \ . \qquad (6) $$

However, in order to validate our camera centering position, we need the reverse, that is, the position ${}^{w}C_k$ of the camera center in the world reference system, and the rotation matrix R_k from the k-th camera reference system to the first. The new subscript k numbers the camera position.

Using the rotation matrix formula (5) with the Euler angles returned by the calibration procedure, we can calculate ${}^{c}_{w}R_k$, the rotation matrix from world coordinates to camera system k. Then, the rotation matrix from coordinates of camera k to coordinates of camera 1 is given by

$$ R_k = {}^{c}_{w}R_1\, {}^{c}_{w}R_k^T \ , \qquad (7) $$

and the k-th camera projection center in the world system is

$$ {}^{w}C_k = -{}^{c}_{w}R_k^T\, {}^{c}O_k . \qquad (8) $$

After finding the rotation matrix, the Euler rotation angles from camera 1 to camera k can be computed by $[\alpha, \beta, \gamma] = [-\arctan(R_{23}/R_{33}), \arcsin(R_{13}), -\arctan(R_{12}/R_{11})]$ where α is the amount of rotation around the x–axis, β is the amount of rotation around the newly rotated y–axis and γ is the amount of rotation around the twice rotated z–axis, all in the counter–clockwise direction.

4. The Intrinsic Camera Model

In this section we summarize the intrinsic camera model used in [11]. Intrinsic calibration is necessary because lenses, especially wide angle ones, introduce distortion, and because the image sensor may not be exactly orthogonal to the optical axis of the lens. Figure 3 shows an image of a black–white checkerboard distorted mildly at the center but severely towards the edges. Next to it are the corners after calibration. The method in [11, 18] performs intrinsic and extrinsic calibration at the same time.

Let a point P in the world have coordinates ${}^{c}P = [x, y, z]^T$ in the camera reference system C–xyz. Under

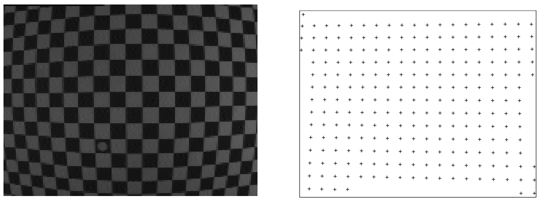

Figure 3. The lens is seriously distorted (left). A calibration must be done (right) first.

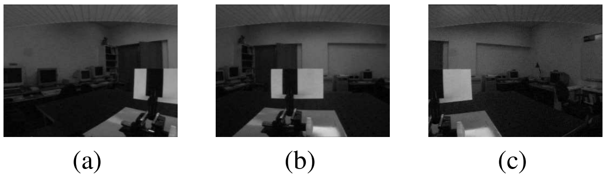

Figure 4. The right side of the black rectangle is aligned with the right side of the dark door in the back. When the camera rotates around an axis through its projection center, the vertical lines stay aligned.

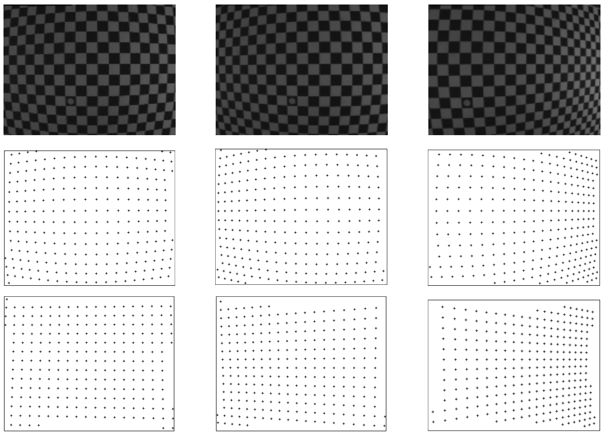

Figure 5. The raw estimates of the corner positions of the checkerboard images at top are depicted in the middle row. The bottom row shows the calibrated corners. The 2nd and 3rd images differ from the 1st (left) column by a rotation of $5°$ and $-15°$.

the idealized pinhole model, P is projected to the image plane with xy coordinates given by

$$\tilde{\mathbf{u}} = \begin{bmatrix} \tilde{u} \\ \tilde{v} \end{bmatrix} = \frac{f}{z} \begin{bmatrix} x \\ y \end{bmatrix}, \tag{9}$$

where f is the camera focal distance. This ideal model is then distorted to

$$d(\tilde{\mathbf{u}}) = \tilde{\mathbf{u}} + \delta(\tilde{\mathbf{u}}) \tag{10}$$

by a radial function around the image center (i.e. principal point) $\mathbf{u}_c = [u_c, v_c]^T$ modeled with a low degree polynomial

$$\delta(\tilde{\mathbf{u}}) = (k_1 r^2 + k_2 r^4)\,\tilde{\mathbf{u}}, \qquad r = ||\tilde{\mathbf{u}}||. \tag{11}$$

Thus, with the pixel aspect ratio s_u and horizontal pixel size D, the final image reading from the camera is

$$\mathbf{u} = \begin{bmatrix} D s_u & 0 \\ 0 & D \end{bmatrix} \tilde{\mathbf{u}} + \mathbf{u}_c. \tag{12}$$

This model is characterized by the intrinsic parameters $\mathbf{I} = [f, s_u, k_1, k_2, D]$.

With measured image points $\mathbf{U}_{ij} = [U_{ij}, V_{ij}]^T$ of calibration target points P_i $(i = 1, \ldots, N)$ in M images $j = 1, \ldots, M$, calibration becomes a minimization problem:

$$\mathbf{I}, \mathbf{E}_1, ..., \mathbf{E}_M = \text{argmin} \sum_{ij} ||\mathbf{U}_{ij} - \mathbf{u}_{ij}||^2 \tag{13}$$

where $\mathbf{E}_k = [{}^cO_k, \alpha_k, \beta_k, \gamma_k]^T$ are the extrinsic camera parameters defined in equation (6). This non–linear least square problem is typically solved with Gauss-Newton or Levenberg–Marquardt methods [5]. In [10], the direct linear transform technique [1, 8, 14] is used to get an initial estimate for an iterative search for these parameters.

5. Image Measurements

Two types of calibration targets are employed in this paper. In the camera centering procedure, a near and a far target are necessary, each with a clearly visible transition from black to white. Figure 4 shows three different pictures of these targets. The second target is a checkerboard pattern used for intrinsic and extrinsic camera calibration. Figure 5 shows three pictures of the checkerboard pattern.

A two dimensional filter matrix F of size 5×5 is used to generate the highest response at the corner points. The center row and column of the filter matrix are filled with zeros. The nonzero elements are then subdivided into four blocks and filled with either 1 for the top left and bottom righ blocks and -1 for the other two blocks. Then, subpixel accuracy is achieved by fitting a quadratic function,

$$q(x, y) = A(x - c_x)^2 + B(y - c_y)^2. \tag{14}$$

For any two fitting points (x_0, y_0) and (x_k, y_k), we have $q(x_k, y_k) - q(x_0, y_0) = [x_k^2 - x_0^2, -2(x_k - x_0), y_k^2 - y_0^2, -2(y_k - y_0)]\eta$ with $\eta = [A, Ac_x, B, Bc_y]^T$. If fitting is performed in a 5×5 window around each point of maximum, a 24×4 linear system is obtained for η and can be solved by least squares. The maximum point (c_x, c_y) of the quadratic function is taken as the final corner point.

6. Experiments

Our image capture system has a Schneider (CNG 1.8/4.8) lens, a Sony (XC-77) CCD camera, and an SGI (Galileo Video) frame grabber. The camera is mounted on a motorized jig (see figure 6), which has five degree of freedom — translations in three directions, plus panning and tilting. The accuracy of motion control of the jig system is $\pm 10^{-2}$ mm and degrees for translations and rotations. An additional, manual xz translation stage is mounted on top of the jig, in order to allow moving the camera's center of projection for the centering procedure described in Section 2. As mentioned in Section 3, the camera coordinate system has its origin at the image projection center, the x–axis is the horizontal direction of pixel reading increasing (right), the y–axis is the vertical direction of pixel reading increasing (down), and the z–axis is formed by the right–hand system convention, so that it points toward the scene. In the following, we describe experiments with the centering procedure, image measurements, and camera calibration. Finally, we show the numerical results of our validation method.

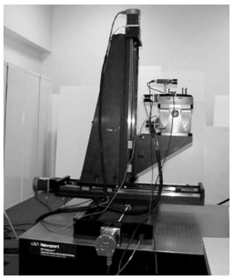

Figure 6. This jig system has 5 motorized degrees of freedom: pan, tilt, and 3 for translation. Two additional, manual degrees of freedom are added for the centering procedure in Section 2.

Centering. After applying the centering procedure in Section 2, different images show essentially no misalignment of the near and far target. Figure 4 shows the alignment of the two vertical lines in three poses: panning $30°$, $0°$ and $-30°$. The front line is about 175 mm away from the camera, whereas the back line is on a wall about 4500 mm away.

Image Measurements. Our calibration control points are from a large checkerboard with $30\text{mm} \times 30\text{mm}$ black and white squares printed with a HP–CM755 large-format ink jet printer. The checkerboard is glued to the back of a large, flat glass mount. We took five images of the checkerboard. In image 1, the image plane is nearly parallel to the checkerboard. The distance from the camera center to the checkerboard was measured to be somewhere between 280 and 305 mm. Image 2 is obtained by a panning of 5 degrees to the left relative to image 1. Thus, camera pose 2 is obtained from camera pose 1 by rotating the camera precisely 5 degrees, and approximately about its y–axis. Camera pose 3 is obtained with a rotation of exactly $15°$ about the approximate y–axis from camera pose 1. Images 4 and 5 are taken after rotations of $-5°$ and $-15°$ from image 1, in the opposite direction with respect to images 2 and 3. The checkerboard corner points in the images are then obtained with the methods described in Section 5. In Figure 5, the top three pictures are images 1, 2 and 5 and the middle three drawings depict the resulting corner points in these images. There are about 235 control points.

	Cam 1	Cam 2	Cam 3	Cam 4	Cam 5
O_k	-66.48	-40.59	11.89	-91.91	-140.4
	112.16	112.03	111.76	112.30	112.56
	294.23	298.96	301.49	287.18	266.79
$\alpha°$	1.6386	1.6527	1.6208	1.6640	1.6968
$\beta°$	1.2692	6.2588	16.284	-3.770	-13.78
$\gamma°$	-0.391	-0.385	-0.367	-0.396	-0.411

Table 1. The raw computation results of camera positions and orientation Euler angles.

Calibration. The computation with code from [10] produces the camera intrinsic parameters: $f = 5.4273$ mm and $s_u = 1.0145$ for focal distance and scaling, $[u_c, v_c] = [317.6943, 231.1014]$ pixels for the image center, and $[k_1, k_2] = [-0.0067, 0.0001]$ for the radial distortion.

The calibrated checkerboard corners for these three displayed checkerboard images are shown in Figure 5 at the bottom row. As expected, the distortion is corrected and straight lines appear straight.

Validation. The results for the extrinsic camera parameters as returned by the calibration algorithm [10] are given in Table 1. The camera projection center positions are the object world origin positions in the camera reference systems. The Euler angles in Table 1 are from the world reference system to the camera reference systems.

According to the calibration image acquisition process, we expect *(i)* the five camera positions to be identical; *(ii)* the camera rotation amounts with respect to camera 1 to be $\pm 5°$ and $\pm 15°$ for images 2–5. To verify these expectations, we computed the coordinate transformations described in Section 3, to obtain camera pose in the world reference system. The resulting Euler angles are displayed in Table 2.

	Cam 1	Cam 2	Cam 3	Cam 4	Cam 5
α°	0	0.0077	-0.0762	0.0191	0.0005
β°	0	4.9877	15.0096	-5.0368	-15.038
γ°	0	-0.1369	-0.4154	0.1402	0.4203

Table 2. Euler angles from camera 1 to other cameras.

	Cam 1	Cam 2	Cam 3	Cam 4	Cam 5
${}^wC_k$	73.743	73.685	73.809	73.605	73.588
	-120.0	-120.2	-120.1	-120.1	-120.2
	-289.4	-289.3	-289.3	-289.3	-289.3
Err	0.0570	-0.001	0.1231	-0.081	-0.098
	0.0772	-0.045	0.0408	-0.009	-0.064
	-0.050	-0.025	0.0509	0.0190	0.0046

Table 3. Camera position components ${}^wC_k$ [mm] in the object world coordinate system and displacements from their centroid [mm].

The rotations around the y–axis are $\pm 5^\circ$ and $\pm 15^\circ$ with an error of 0.04° or less, just as we hoped.

The results in Table 3 indicate that the camera centers of projection are practically in the same position, to within 0.12 mm or less from their centroid. As a last sanity check, notice that the distance from camera center to the target plane is about 289.3 mm, well inside the manually measured range of 280–305 mm.

All these results indicate that the camera's center of projection has been positioned very accurately along the rotation axis of the rotation platform, and that our error estimate of 0.1 millimeters for eccentricity is plausible.

7. Conclusions and Acknowledgements

We designed a process to align the projection center of a camera to a rotation axis, so that multiple images can be taken from a fixed projection center with different orientations. Experimental results with wide angle lens with severe lens distortion are consistent and satisfactory, and determine camera centering to be accurate within a tenth of a millimeter, as validated by a precision jig. A description of the centering and calibration procedures, as well as images, data, and Matlab code will be accessible through the world-wide web [21].

This research was supported under NSF Grants IRI-9201751 and IRI-9496205. The authors thank Cindy Chen, James Davis, Joachim Hornegger, Li–Yi Wei, Yossi Rubner and Mark Ruzon for discussions.

References

[1] Y. I. Abdel-Aziz and H. M. Karara. Direct linear transformation into object space coordinates in close–range photogrammetry. In *Proceedings of the Symposium on Close–Range Photogrammetry, Urbana, IL*, pages 1–18, 1971.

[2] P. Beardsley, D. Murray, and A. Zisserman. Camera calibration using multiple images. In *ECCV92*, pages 312–320, 1992.

[3] T. Brodsky, C. Fermuller, and Y. Aloimonos. Self-calibration from image derivatives. In *ICCV98*, pages 83–89, 1998.

[4] J. Craig. *Introduction to robotics: mechanics and control.* Addison-Wesley, 2nd edition, 1989.

[5] J. Dennis, Jr. and R. B. Schnabel. *Numerical methods for unconstrained optimization and nonlinear equations*. Englewood Cliffs, N.J. : Prentice-Hall, 1983.

[6] O. Faugeras, Q. Luong, and S. Maybank. Camera self-calibration: Theory and experiments. In *ECCV92*, pages 321–334, 1992.

[7] O. Faugeras, L. Quan, and P. Sturm. Self-calibration of a 1-d projective camera and its application to the self-calibration of a 2-d projective camera. In *ECCV98*, pages 36–52, 1998.

[8] O. Faugeras and G. Toscani. Camera calibration for 3d camputer vision. In *Proceedings International Workshop on Industrial Applications of Machine Vision and Machine Intelligence, Skilken, Japan*, pages 204–247, 1987.

[9] R. Hartley. Self-calibration of stationary cameras. *IJCV*, 22(1):5–23, February 1997.

[10] J. Heikkilä. Calibration matlab code. In *http://ee.oulu.fi/∼jth*, 1997.

[11] J. Heikkilä and O. Silvén. A four-step camera calibration procedure with implicit image correction. In *Proceedings of the IEEE Conference on Computer Vision and Patter Recognition*, pages 1106–1112, 1997.

[12] A. Heyden and K. Astrom. Euclidean reconstruction from image sequences with varying and unknown focal length and principal point. In *CVPR97*, pages 438–443, 1997.

[13] J. Kearney, X. Yang, and S. Zhang. Camera calibration using geometric constraints. In *CVPR89*, pages 672–679, 1989.

[14] T. Melen. Geometrical modelling and calibration of video cameras for underwater navigation. Doctor thesis, Norges tekniske høgskole, Institutt for teknisk kybernetikk, 1994.

[15] T. Pajdla and V. Hlavac. Camera calibration and 3D Euclidean reconstruction from known observer translations. In *CVPR98*, pages 421–426, 1998.

[16] M. Pollefeys, R. Koch, and L. VanGool. Self-calibration and metric reconstruction in spite of varying and unknown internal camera parameters. In *ICCV98*, pages 90–95, 1998.

[17] B. Rousso and E. Shilat. Varying focal length self-calibration and pose estimation. In *CVPR98*, pages 469–474, 1998.

[18] C. C. Slama. *Manual of Photogrammetry*. Am. Soc. of Photogrammetry, 4th edition, 1980.

[19] G. Stein. Lens distortion calibration using point correspondences. In *CVPR97*, pages 602–608, 1997.

[20] R. Tsai. A versatile camera calibration technique for high-accuracy 3d machine vision metrology using off-the-shelf tv cameras and lenses. *IEEE Journal of Robotics and Automation*, 3(4):323–344, 1987.

[21] J. Zhang. Matlab code. In *http://vision.stanford.edu/∼zhang*.